Inorg. Chem. **1991**, *30*, 1345–1353 **1345**

Contribution from the Department of Chemistry, Virginia Commonwealth University, Box 2006, Richmond, Virginia 23284,
Institute of Pharmaceutical Chemistry, University of Milano, Viale Abruzzi 42, 20100 Milano, Italy,
and Institute of Chemistry and Technology of Radioelements, CNR, Corso Stati Uniti 4, 35100 Padova, Italy

Complexes of the Lanthanide(III) Ions with an Aromatic Six-Nitrogen-Donor Macrocyclic Ligand

F. Benetollo,[1a] G. Bombieri,[1b] K. K. Fonda,[1c] A. Polo,[1c] J. R. Quagliano,[1c,d] and L. M. Vallarino*,[1c]

Received June 14, 1990

A series of complexes of formula $ML^3X_3 \cdot nS$, in which M is La(III)–Yb(III), L^3 is $C_{26}H_{18}N_6$, X is a mononegative ion, and S is water or methanol, were obtained by metal-templated condensation from 2,6-diformylpyridine and 1,2-diaminobenzene, as well as by metal exchange from $Ba(L^3)_2(ClO_4)_2$. The spectral properties of the complexes (IR and ^1H and ^{13}C NMR spectra for the diamagnetic species) closely resembled those of the Sr(II) analogue, the structure of which was established by X-ray analysis. The latter compound consisted of two slightly different entities, $SrL^3(CF_3SO_3)_2$ and $SrL^3(CF_3SO_3)_2 \cdot H_2O$, present in a 1:1 ratio and both containing a Sr(II) surrounded by the six nitrogen-donor atoms of an 18-member macrocyclic ligand. The lanthanide–macrocycle entities were found to be remarkably inert to metal release in solution, whereas the exocyclic ligands (anions and solvent) were labile and easily exchanged. The major organic byproduct of the metal-templated syntheses was identified as 2,6-bis(2-benzimidazolyl)pyridine.

Introduction

The ability of the lanthanide(III) ions to promote the Schiff-base condensation of appropriate diamine and dicarbonyl precursors, resulting in the formation of metal complexes of otherwise inaccessible macrocyclic ligands, is by now well established, and the topic was recently reviewed.[2-4] Most efforts to date have focused on symmetric macrocycles consisting of two identical aromatic head units (pyridines,[5-14] furans,[15,16] or phenols[17-23]) symmetrically connected through imine linkages to identical aliphatic side chains. The complexes of the 18-member, six-nitrogen-donor ligands L^1[8,9] and L^2[5-7,10-14] (Figure 1a) have received special attention because of their unique inertness toward metal release in solution, even under conditions that would result in the immediate decomposition of most other lanthanide complexes. In contrast, little has been reported on lanthanide macrocycles having rigid, aromatic side chains. Trinitrate complexes of the larger lanthanides (La–Nd) with the aromatic tetraaldimine L^3 (Figure 1b) were obtained by Gray and Hart[24] by transmetalation from the corresponding bimacrocyclic complex of barium perchlorate.[25] More recently, we reported the only well-characterized examples of metal complexes of the aromatic tetraketoimine L^4 (Figure 1b), obtained by metal-templated synthesis with the nitrates of the larger lanthanides, La–Nd.[26] The true macrocyclic structure of these L^4 complexes was established by single-crystal X-ray analysis of a praseodymium dinitrate–perchlorate species.

The isolation and unambiguous identification of complexes of the L^4 macrocycle[26] were significant because contrasting earlier reports[27-31] had cast serious doubt on the very existence of this ligand. However, the practical value of the synthesis was limited by very low yields; furthermore, the synthesis could not be usefully extended from neodymium to the only slightly smaller europium. We were intrigued by this failure, which appeared to result chiefly from the competing facile formation of the metal-free methylene-bridged isomer[28] of L^4. We also had a special interest in obtaining a macrocyclic complex of Eu with *o*-phenylenediimine side chains and pyridine head units, because we hoped that such a highly aromatic complex would exhibit an inertness comparable to that of its aliphatic L^1 and L^2 analogues, together with a more intense ligand-mediated luminescence.[2] Therefore, we set out to investigate systematically the lanthanide-templated synthesis of the complexes of ligand L^3, for which there could be no competitive cyclization involving methyl groups. Also, in order to extend the very limited structural knowledge available for L^3–metal complexes (only two structures reported[33]), we carried out a single-crystal X-ray analysis of the Sr–L^3 triflate complex, previously synthesized by Drew et al.[33]

Experimental Section

Starting Materials and Procedures. 2,6-Pyridinedicarboxyaldehyde and 1,2-diaminobenzene were obtained from Aldrich Chemical Co.; the diamine was sublimed prior to use. Lanthanide(III) nitrates and acetates

---

(1) (a) Institute of Chemistry and Technology of Radioelements. (b) University of Milano. (c) Virginia Commonwealth University. (d) Current address: Department of Chemistry, University of Virginia, Charlottesville, VA.

(2) Bombieri, G. *Inorg. Chim. Acta* **1987**, *139*, 21.

(3) Fenton, D. E.; Vigato, P. A. *Chem. Soc. Rev.* **1988**, *17*, 69.

(4) Vallarino, L. M. *J. Less-Common Met.* **1989**, *149*, 121.

(5) Backer-Dirks, J. D. J.; Gray, C. J.; Hart, F. A.; Hursthouse, M. B.; Schoop, B. C. *J. Chem. Soc., Chem. Commun.* **1979**, 774.

(6) Radecka-Paryzek, W. *Inorg. Chim. Acta* **1980**, *45*, L147.

(7) Wang, G.; Miao, L. *Gaodeng Xuexiao Huaxue Xuebao* **1984**, *5* (3), 281; *Chem. Abstr.* **1984**, *101*, 182591c.

(8) Abid, K. K.; Fenton, D. E. *Inorg. Chim. Acta* **1984**, *95*, 119.

(9) Abid, K. K.; Fenton, D. E.; Casellato, U.; Vigato, P. A.; Graziani, R. *J. Chem. Soc., Dalton Trans.* **1984**, 351.

(10) De Cola, L.; Smailes, D. L.; Vallarino, L. M. *Inorg. Chem.* **1986**, *25*, 1729.

(11) Bombieri, G.; Benetollo, F.; Polo, A.; De Cola, L.; Smailes, D. L.; Vallarino, L. M. *Inorg. Chem.* **1986**, *25*, 1127.

(12) Arif, A. M.; Backer-Dirks, J. D. J.; Gray, C. J.; Hart, F. A.; Hursthouse, M. B. *J. Chem. Soc., Dalton Trans.* **1987**, 1665.

(13) Bombieri, G.; Benetollo, F.; Polo, A.; De Cola, L.; Hawkins, W. T.; Vallarino, L. M. *Polyhedron* **1989**, *8*, 2157.

(14) Bombieri, G.; Benetollo, F.; Hawkins, W. T.; Polo, A.; Vallarino, L. M. *Polyhedron* **1989**, *8*, 1923.

(15) Abid, K. K.; Fenton, D. E. *Inorg. Chim. Acta* **1984**, *82*, 223.

(16) Zang, Y.; Wang, D.; Wang, G.; Zeng, C. *Wuji Huaxue* **1987**, *3*, 66; *Chem. Abstr.* **1987**, *107*, 227850d.

(17) Kahwa, A.; Selbin, J.; Hsieh, T. C.-Y.; Lane, R. A. *Inorg. Chim. Acta* **1986**, *118*, 179.

(18) Zanello, P.; Cinquantini, A.; Guerriero, P.; Tamburini, S.; Vigato, P. A. *Inorg. Chim. Acta* **1986**, *117*, 91.

(19) Sakamoto, M. *Bull. Chem. Soc. Jpn.* **1987**, *60*, 1546.

(20) Bullita, E.; Casellato, U.; Guerriero, P.; Vigato, P. A. *Inorg. Chim. Acta* **1987**, *139*, 59.

(21) Guerriero, P.; Casellato, U.; Tamburini, S.; Vigato, P. A.; Graziani, R. *Inorg. Chim. Acta* **1987**, *129*, 127.

(22) Bullita, E.; Guerriero, P.; Tamburini, S.; Vigato, P. A. *J. Less-Common Met.* **1989**, *153*, 211.

(23) Bünzli, J.-C.; Moret, E.; Casellato, U.; Guerriero, P.; Vigato, P. A. *Inorg. Chim. Acta* **1988**, *150*, 133.

(24) Gray, C. J.; Hart, F. A. *J. Chem. Soc., Dalton Trans.* **1987**, 2289.

(25) Cabral, J. O.; Cabral, M. F.; Cummins, W. J.; Drew, M. G. B.; Rodgers, A.; Nelson, S. M. *Inorg. Chim. Acta* **1978**, *30*, L313.

(26) Benetollo, F.; Bombieri, G.; De Cola, L.; Polo, A.; Smailes, D. L.; Vallarino, L. M. *Inorg. Chem.* **1989**, *28*, 3447.

(27) Stotz, R. W.; Stoufer, R. C. *J. Chem. Soc., Chem. Commun.* **1970**, 1682.

(28) Cabral, J. O.; Cabral, M. F.; Drew, M. G. B.; Esho, F. S.; Haas, O.; Nelson, S. M. *J. Chem. Soc., Chem. Commun.* **1982**, 1066.

(29) Radecka-Paryzek, W. *Inorg. Chim. Acta* **1981**, *54*, L251.

(30) Radecka-Paryzek, W. *Inorg. Chim. Acta* **1985**, *109*, L21.

(31) Zhang, R.; Tong, B. *Huaxue Tongbao* **1986**, *2*, 35; *Chem. Abstr.* **1986**, *104*, 236176d.

(32) Sabbatini, N.; De Cola, L.; Vallarino, L. M.; Blasse, G. *J. Phys. Chem.* **1987**, *18*, 4681.

(33) Drew, G. B.; Cabral, J. O.; Cabral, M. F.; Esho, F. S.; Nelson, S. M. *J. Chem. Soc., Chem. Commun.* **1979**, 1033.

0020-1669/91/1330-1345$02.50/0

Table I. Macrocyclic Complexes and Infrared Absorptions (cm^{-1}) of Anions

complex	method of prep[a]	selected absorptions and assignments[b]	
		Trinitrates	
$LaL^3(NO_3)_3\cdot 1.5H_2O$	1–3	1443 vs, b (ν_5); 1335, 1310 vs, b (ν_1);[c] 1008 m (ν_2)	N–O stretching modes of coord NO_3^-
$CeL^3(NO_3)_3\cdot H_2O$	1	1435 vs, b (ν_5); 1340 vs, b, 1310 sh (ν_1);[c] 1010 m (ν_2)	
$PrL^3(NO_3)_3\cdot 1.5H_2O$	1, 3	1443 vs, b (ν_5); 1331, 1330 vs, b (ν_1);[c] 1002 m (ν_2)	
$NdL^3(NO_3)_3\cdot 4.5H_2O$	1	1445 vs, b (ν_5); 1340, 1310 vs, b (ν_1);[c] 1005 m (ν_2)	
$SmL^3(NO_3)_3\cdot H_2O$	1	1443 vs, b (ν_5); 1337, 1302 vs, b (ν_1);[c] 1002 m (ν_2)	
$EuL^3(NO_3)_3$	1, 3	1445 vs, b (ν_5); 1340, 1315, 1290 vs, b (ν_1);[c] 1002 m (ν_2)	
$GdL^3(NO_3)_3$	1	1445 vs, b (ν_5); 1345, 1320, 1290 vs, b (ν_1);[c] 1000 m (ν_2)	
		Others	
$SrL^3(CF_3SO_3)_2\cdot 1.5H_2O$	1	1275, 1289 vs, b [$\nu(SO_3)(E)$]; 1159 vs [$\nu(CF_3)(E)$]; 1028 vs [$\nu(SO_3)(A_1)$]; 637 s [$\delta(SO_3)(A_1)$], 519 m [$\delta(CF_3)(E)$, $\delta(SO_3)(E)$]	
$LaL^3(CF_3SO_3)_3\cdot H_2O$	1	1301–1166 vvs, vb with maxima at 1301, 1275, 1235, 1166 [$\nu(SO_3)(E)$, $\nu(CF_3)(E)$]; 1029 vs [$\nu(SO_3)(A_1)$]; 637 vs [$\delta(SO_3)(A_1)$]; 512 m [$\delta(CF_3)(E)$, $\delta(SO_3)(E)$]	
$EuL^3(CF_3SO_3)_3\cdot 2H_2O$	1	1316–1168 vvs, vb with maxima at 1316, 1279, 1240, 1168 [$\nu(SO_3)(E)$, $\nu(CF_3)(E)$]; 1029 vs [$\nu(SO_3)(A_1)$]; 635 vs [$\delta(SO_3)(A_1)$]; 516 m [$\delta(CF_3)(E)$, $\delta(SO_3)(E)$]	
$Ba(L^3)_2(ClO_4)_2$		1091 vs, b (ν_3); 626 s (ν_4)	Cl–O antisym stretching and bending modes of ionic ClO_4^-
$Ba(L^3)_2(ClO_4)_2\cdot 1.5H_2O$		1090 vs, b (ν_3); 626 s (ν_4)	
$LaL^3(ClO_4)_2(OH)\cdot 1.5H_2O$[d]	2	1080 vs, b (ν_3); 625 m (ν_4)	
$LaL^3(CH_3COO)_3\cdot 2.5CH_3OH\cdot 3.5H_2O$	1	1567 vvs, b; 1415 vs, b	stretching modes of $-COO^-$ group
$CeL^3(CH_3COO)_3\cdot 5H_2O$	1	1465 vs, b; 1410 vs, b	
$CeL^3(CH_3COO)_2(ClO_4)\cdot H_2O$	2	1531 vs, 1451 vs, 1418 s ($\nu(COO^-)$); 1104 vs, b (ν_3), 623 (ν_4) (ionic ClO_4^-)	
$TbL^3(NO_3)_{1.5}(OH)_{1.5}\cdot 0.5H_2O$[d]	1	1467 s, b (ν_5); 1380, 1345 vs, b, 1279 s (ν_3, ν_1)	N–O stretching modes of coord (ν_5, ν_1) and ionic (ν_3) NO_3
$DyL^3(NO_3)_{1.5}(OH)_{1.5}\cdot 1.5H_2O$[d]	1	1467 s, b (ν_5); 1380, 1345 vs, b,[c] 1280 s (ν_3, ν_1)	
$ErL^3(NO_3)_{1.5}(OH)_{1.5}$[d]	1	1470 s, b (ν_5); 1375, 1340 vs, b,[c] 1300 sh, 1280 s (ν_3, ν_1)	
$YbL^3(NO_3)_2(OH)\cdot H_2O$[d]	1	1500 vs (ν_5); 1390, 1345 vs, b,[c] 1295 s (ν_3, ν_1)	
$LaL^3(NO_3)_{1.75}(Cl)_{1.25}\cdot 1.5H_2O$	2	1443 vs, b (ν_5); 1314 vs, b[c] (ν_1); 1002 m (ν_2)	N–O stretching modes of coord NO_3^-
$HoL^3(NO_3)_{1.75}(Cl)_{1.25}\cdot H_2O$	4	1519 vs (ν_5); 1277 (ν_1); 1007 m-w (ν_2)	
$HoL^3(NO_3)_2(ClO_4)\cdot CH_3OH$	4	1517 vs (ν_5); 1281 (ν_1) (coord NO_3^-), 1102 vs, b (ν_3); 623 m (ν_4) (ionic ClO_4^-)	
$TmL^3(SCN)_2(ClO_4)\cdot 2H_2O$	4	2050 vs ($\nu(C{\equiv}N)$) (NCS^-); 1090 m (ν_3), 620 m (ν_4) (ionic ClO_4^-)	

[a] 1 = metal-template synthesis; 2 = metal-template synthesis followed by anion exchange; 3 = simple transmetalation from $Ba(L^3)_2(ClO_4)_2$; 4 = transmetalation from $Ba(L^3)_2(ClO_4)_2$ in the presence of added anions and/or followed by anion exchange. [b] s = strong, m = medium, w = weak, v = very, and b = broad. Notations used in the assignments follow ref 40 for all anions except $CF_3SO_3^-$, where ref 43 was followed. [c] Broad absorption with partly resolved maxima. [d] The $\nu(OH)$ absorption appears as a broad band near 3250 cm^{-1}.

Table II. Proton NMR Spectral Data for Diamagnetic Complexes

	chem shifts, ppm vs TMS		
complex	H—C=N	pyridine	benzene
$LaL^3(NO_3)\cdot 1.5H_2O$[a]	9.33 s, 4 H	8.57 t, 8.33 d, *J* = 7.8 Hz, 6 H	7.94, 7.71, 1:1 mult,[b] 8 H
$LaL^3(CF_3SO_3)_3\cdot H_2O$	9.96 s, 4 H	9.00 overlapping mult, 6 H	8.54, 8.35, 1:1 overlapping mult, 8 H
$SrL^3(CF_3SO_3)_2\cdot 1.5H_2O$	9.21 s, 4 H	8.45 t, 8.22 d, *J* = 7.8 Hz, 6 H	7.87, 7.64, 1:1 mult, 8 H
$PbL^3(ClO_4)_2$	9.72 s, 4 H	8.56 t, 8.33 d, *J* = 7.5 Hz, 6 H	7.88, 7.72, 1:1 mult, 8 H
$BaL^3(ClO_4)_2$	8.55 s, 4 H	8.08 t, 7.68 d, *J* = 7.8 Hz, 6 H	7.19, 7.15, 1:1 mult, 8 H

[a] Spectrum coincides with that reported in ref 24. [b] mult = multiplets.

Table III. Carbon-13 NMR Spectral Data for Diamagnetic Complexes

	chem shifts, ppm vs TMS						
		pyridine			benzene		
complex	C^1	C^2	C^3	C^4	C^5	C^6	C^7
$SrL^3(CF_3SO_3)_3\cdot 1.5H_2O$	161.68	153.11	131.34	141.52	144.44	130.90	120.28
$KL^3(ClO_4)\cdot H_2O$	159.35	153.46	129.25	139.46	144.29	128.69	118.52
$Ba(L^3)_2(ClO_4)_2$	160.33	152.58	130.09	139.80	143.49	129.08	118.13
$PbL^3(ClO_4)_2$	160.59	152.57	131.12	140.98	143.25	130.36	119.52
$LaL^3(NO_3)_3\cdot 1.5H_2O$	162.17	151.64	131.27	141.35	143.55	130.27	119.59
$LaL^3(CF_3SO_3)_3\cdot H_2O$	162.43	152.46	131.99	142.17	144.01	130.90	120.28

were purchased from Alpha Products-Thiokol and stored over P_4O_{10}. The triflates were prepared by dissolving the metal oxides in aqueous trifluoromethanesulfonic acid and evaporating the solutions to dryness in a rotary evaporator under reduced pressure. The white solids thus formed were filtered out, washed with diethyl ether, recrystallized from acetonitrile, and dried in vacuo over P_4O_{10}. The solvents (Aldrich, reagent or spectral grade) were used without further purification.

Thermogravimetric analyses (TGA) were carried out on a Perkin-Elmer TGS-2 thermogravimetric system under a dry-He flow of 60 mL min^{-1}. Infrared (IR) spectra were recorded on a Perkin-Elmer 1600 FT-IR spectrophotometer, in the range 4000–450 cm^{-1}; samples were examined as KBr pellets as well as Nujol–hexachlorobutadiene mulls. Fluorescence spectra were measured at room temperature with a SLM-8000 spectrofluorometer. Nuclear magnetic resonance (NMR) spectra were obtained with a General Electric QE-300 Fourier transform spectrometer, using dimethyl sulfoxide-d_6, chloroform-*d*, and deuterium oxide (Aldrich) as solvents. Powdery samples were examined for crystallinity with an ISI DS-130S scanning electron microscope. Microanalyses (C, H, N) were performed by Atlantic Microlab, Atlanta, GA, and Galbraith Laboratories, Knoxville, TN. Unit resolution mass spectral measurements (electron impact) were made on a Finnegan MAT-4600 GC/MS spectrometer with perfluorotributylamine (FC 43) as a peak-matching standard.

Synthesis and Characterization of the Complexes. The complexes are listed in Table I, together with their method of preparation and IR absorptions of the anions. ^1H and ^{13}C NMR spectra are given in Tables II and III.

Lanthanide-Templated 2:2:1 Condensation. Both the handling of the organic precursors and the condensation reaction were carried out in a dry nitrogen atmosphere.

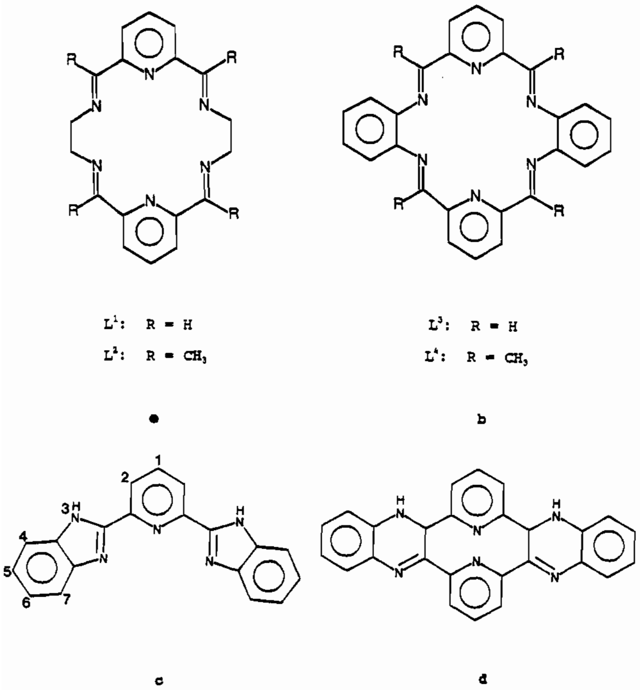

Figure 1. Hexaaza macrocyclic ligands (a, b), principal organic byproduct 2,6-bis(2-benzimidazolyl)pyridine (c), and secondary organic byproduct $C_{26}H_{18}N_6$ (d).

The trinitrate and nitrate–hydroxide complexes were obtained as follows: 1,2-Diaminobenzene (2.0 mmol) and the hydrated lanthanide nitrate (1.0 mmol) were dissolved in anhydrous methanol (30 mL) at room temperature, and 2,6-pyridinedicarboxyaldehyde (2.0 mmol in 20 mL of methanol) was added all at once, with stirring. The mixture was refluxed for 4 h, during which time the color of the solution changed from orange to yellow; a bright yellow microcrystalline precipitate gradually formed. The nitrogen flow was discontinued, and the solid was filtered off with suction, washed on the filter with methanol and chloroform, and dried in vacuo over P_4O_{10}. The product thus isolated could not be recrystallized owing to lack of solubility in suitable solvents; however, it was usually homogeneous under a microscope and appeared to be pure by microanalysis and IR spectroscopy. A second crop of product of lesser purity was obtained by concentrating the mother liquor to approximately half of the original volume in a rotary evaporator under reduced pressure, followed by chilling at 0 °C for several hours. Approximate total yields: La–Nd, 70–80%; Sm–Gd, 50–60%; Tb, 40%. Starting at Dy, yields became erratic and decreased sharply, being less than 5% for Lu. The complexes of Ho, Tm, and Lu, which had IR spectra identical with that of the Tb complex but gave slightly incorrect analyses (carbon ca. 1% too high), were not listed in Table I.

The tritriflate and triacetate complexes were obtained as described for the nitrates, except that the triflate reactions were carried out in acetonitrile. For the acetates, concentration of the reaction mixture was necessary to precipitate the products. These were recrystallized several times, the triflates from acetonitrile–diethyl ether and the acetates from chloroform–diethyl ether. Yields were 50–40% for the lanthanum and europium triflates and for the lanthanum and cerium acetates. Other lanthanide acetates gave mixtures from which the macrocyclic complexes, identified by IR spectra, could not be isolated in a pure form.

After isolation of the complexes, evaporation of the yellow-orange mother liquor under reduced pressure produced a dark residue that solidified upon workup with chilled diethyl ether. Repeated fractional crystallization of this solid from methanol–diethyl ether yielded a series of powdery fractions with colors ranging from white to orange-brown. The chloroform-soluble white fraction was purified by column chromatography over basic alumina–$CHCl_3$ and identified as 2,6-bis(2-benzimidazolyl)pyridine[34] (Figure 1c) on the basis of microanalysis, mass spectrometry (parent peak, m/z 311), and ^1H NMR spectroscopy. ^1H chemical shifts in DMSO-d_6 (ppm vs TMS, J values in hertz, assignments refer to Figure 1c): (1) 8.19 t, $J = 7.8$, 1 H; (2) 8.36 d, $J = 7.8$, 2 H; (3) 13.03 br s, 2 H; (4–7) 7.77 and 7.34, br m, 8 H. IR absorptions (cm^{-1}): 3200 m, br, 3060 m, 2931 w, 1596 m, 1572 s, 1458 vvs, 1434 vs, 1390 sh, 1317 s, 1276 m, 1229 w, 1152 w, 1114 vw, 1084 vw, 1005 vw, 996 w, 960 vvw, 930 vvw, 900 vvw, 845 sh, 820 m, 738 vvs, 673 vvw, 552 vvw, 630 vvw, 562 w, br, 520 sh. The compound showed a very intense purple glow when irradiated with UV light. The emission spectrum in chloroform consisted of a broad band (360–420 nm, excitation at 320 nm); the absorption spectrum showed a broad band at 260–340 nm. Reaction of 2,6-bis(2-benzimidazolyl)pyridine with HCl in methanol–diethyl ether produced the hydrochloride as a white powder, with a strong bluish glow under UV irradiation (emission 370–450 nm, λ_{max} = 395 nm, excitation 330 nm). IR absorptions (cm^{-1}): 3389 s, br, 2650 midpoint of vs structured band, 1708 vw, 1614 m-s, 1595 m-s, 1575 w, 1513 s, 1472 vs, 1443 s, 1367 vs, 1308 m, 1261 m, 1232 m-s, 1179 w, 1149 w, 1094 vw, 992 w, 895 w, br, 878 m, br, 744 vs, 615 m-s, 568 m-s, 503 m. ^1H NMR chemical shifts in DMSO-d_6 (ppm vs TMS, J values in hertz, assignments refer to Figure 1c): (1) 8.48 t, $J = 7.8$, 1 H; (2) 8.68 d, $J = 7.8$, 2 H; (3) not seen; (4–7) 7.89 and 7.56 br m, 8 H.

The colored fractions of the residue were investigated by microanalysis, IR and ^1H NMR spectroscopy, and luminescence. They were found to be mixtures containing 2,6-bis(2-benzimidazolyl)pyridine, both free-base and protonated, in nonstoichiometric association with metal salts. Treatment of these mixtures with triethylamine in warm chloroform, followed by column chromatography on basic alumina and evaporation to dryness, yielded pure 2,6-bis(2-benzimidazolyl)pyridine.

Metal-Templated 4:4:1 Condensation with Europium Nitrate and Cerium Acetate. The reaction was carried out as described for the 2:2:1 condensation, except that the precursors-to-metal ratio was doubled. A white solid (less than 10% of the total) separated first from the reaction mixture. The monomacrocyclic europium trinitrate and cerium triacetate complexes were isolated upon further concentration in 30–40% yields. The remaining products were mixtures consisting chiefly of 2,6-bis(2-benzimidazolyl)pyridine and its derivatives, as described for the 2:2:1 condensation. No formation of bimacrocyclic complexes was observed.

The first product of the reaction, white needles from methanol–ether, mp > 270 °C, had molecular formula $C_{26}H_{18}N_6$, as shown by microanalysis and mass spectrometry (parent peak, m/z 414). This compound was assigned the structure shown in Figure 1d. IR absorptions (cm^{-1}): 3049 w, 2943 w, 2890 vvw, 1609 vw, 1578 s, 1455 vs, 1428 m, 1401 m, 1373 s, 1346–1326 m, 1273 m, 1258 w, 1155 m-s, 1073 m-w, 1022 w, 954 vw, 929 vvw, 891 w, 814 m-w, 792 w, 753 sh, 732 vvs, 684 vvw, 674 vvw, 597 w, 561 w, 523 w. ^1H NMR chemical shifts (ppm, J values in hertz): (py) 7.91 d, $J = 8.1$, 2 H, 7.86 d, $J = 7.8$, 2 H, 7.40 t, $J = 7.8$, 2 H; (bz) 7.76 d, $J = 12.9$, 2 H, 7.50 dd, $J = 7.2, 7.2$, 2 H, 7.47 dd, $J = 7.2, 7.2$, 2 H; (NH) 6.21 br s.

Template Synthesis of the Barium Perchlorate, Lead Perchlorate, and Strontium Triflate Complexes. These were prepared as described in the literature and had correct analyses for $Ba(L^3)_2(ClO_4)_2$,[25] $PbL^3(ClO_4)_2$,[33] and $SrL^3(CF_3SO_3)_2{\cdot}nH_2O$ (n = 0.5, 1.5).[35] The Sr complex, recrystallized from acetonitrile–diethyl ether, gave crystals suitable for X-ray analysis.

Safety Note. Reactions involving these and other perchlorate complexes were carried out on small quantities (100–200 mg) and with screen protection, owing to the potential danger of explosion.

Metal-Exchange Reactions from $Ba(L^3)_2(ClO_4)_2$. All reactions were carried out by the same general procedure. Solid $Ba(L^3)_2(ClO_4)_2$ (5×10^{-5} mol) was suspended in anhydrous methanol or acetonitrile (20 mL), and the substituent metal salt (2×10^{-4} mol) was added. The mixture was stirred at 50 °C for several hours; contact with moist air was avoided. The results varied depending on the substituent salt. When this was a nitrate of a larger lanthanide (La–Eu) in methanol, the reaction mixture remained heterogeneous. The color of the suspended solid changed from orange to yellow, with the exact shade depending on particle size. The products were filtered out with suction, washed on the filter with methanol, and dried over P_4O_{10} (yields 80–90%). The compounds thus obtained were the trinitrate complexes, as described by Gray and Hart for the La–Nd species;[24] they were identical with the product of the metal-templated condensation. With the nitrates of the smaller lanthanides (Dy–Yb), a yellow solution resulted from which no pure complex could be isolated by concentration. Addition of an excess of NaSCN or $LiNO_3$ to the concentrated solutions caused precipitation of the lanthanide complexes (30–50% yields) as mixed thiocyanate–perchlorates or nitrate–perchlorates, respectively. The latter had correct IR spectra but were contaminated by minor quantities of simple metal salts and were not listed in Table I. When the bimacrocyclic Ba complex was heated with an excess of hydrated $Ba(ClO_4)_2$ in methanol or acetonitrile, the original complex was recovered as $Ba(L^3)_2(ClO_4)_2{\cdot}H_2O$.

All solutions obtained from the transmetalation reactions showed a purple glow when exposed to UV light. The solutions were taken to dryness under reduced pressure, and the residues were extracted with hot

---

(34) Addison, A. W.; Burke, P. J. *J. Heterocycl. Chem.* **1981**, *18*, 803.

(35) Bell, T. W.; Guzzo, F. *J. Chem. Soc., Chem. Commun.* **1986**, 769.

Table IV. Crystallographic Data for $Sr_2S_4F_{12}O_{13}N_{12}C_{56}H_{38}$

formula	$Sr_2S_4F_{12}O_{13}N_{12}$-$C_{56}H_{38}$	γ, deg	110.44 (3)
M_r	1618.45	Z	2
		ρ_{calcd}, g cm^{-3}	1.67
space group	$P\bar{1}$ (No. 2)	radiation (λ, Å)	Mo Kα (0.71069)
a, Å	19.070 (3)	T, °C	20
b, Å	17.222 (3)	$R = R(F_o)$	0.055
c, Å	11.120 (2)	$R_w = R_w(F_o)$	0.057
α, deg	108.26 (3)	μ(Mo Kα), cm^{-1}	18.25
β, deg	90.61 (2)	V, Å^3	3220.08

chloroform. A minute quantity of 2,6-bis(2-benzimidazolyl)pyridine was isolated by evaporation of the combined chloroform extracts.

Electron Microscope Examination. Complexes that appeared as powders under an optical microscope were examined with an electron microscope. All samples appeared homogeneous and crystalline (needles or prisms), except for the cerium triacetate complex, which consisted of glassy spherules 60–80 μm in diameter.

Solubility and Behavior toward Acids, Bases, and Competing Anions. The tritriflate and triacetate complexes were soluble in methanol, acetonitrile, chloroform, and other polar organic solvents; they were insoluble in nonpolar organic solvents and water. The nitrate–perchlorate species, as first obtained from Ba transmetalation, were very soluble in polar organic solvents as well as water. All other complexes were insoluble or only very sparingly soluble in most organic solvents and water; they dissolved to a limited extent in dimethyl sulfoxide.

The trinitrates (La–Gd), insoluble in methanol alone, dissolved in warm methanol containing NaOH (complex-to-NaOH mole ratio ca. 1:4). The resulting pale yellow solutions remained clear for ca. 30 min, after which time olive green decomposition products precipitated. Neutralization of the freshly prepared basic solutions with nitric acid in methanol regenerated the original trinitrates without appreciable degradation. Addition of $LiClO_4$ to the basic solutions caused precipitation of the perchlorate–hydroxides as tiny yellow crystals. The La species was analyzed and is listed in Table I; the corresponding Pr, Nd, and Eu complexes were characterized by IR spectra.

The lanthanum triflate, lanthanum acetate, and cerium acetate complexes were dissolved in methanol and treated with a 10-fold excess of $LiNO_3$. The corresponding trinitrate complexes precipitated immediately as yellow microcrystals. The lanthanum trinitrate, cerium triacetate, europium tritriflate, and crude holmium nitrate–hydroxide complexes were suspended/dissolved in methanol containing a 10-fold excess of concentrated HCl. After several days at room temperature, the undissolved solids were isolated and the dissolved complexes were precipitated by addition of diethyl ether. Recovery was nearly quantitative; in each case the product was shown by IR spectroscopy (and NMR spectroscopy for La) to contain the unchanged metal–L^3 moieties. However, partial or complete anion metathesis resulted; the lanthanum trinitrate was recovered as a nitrate–chloride, the cerium triacetate and europium tritriflate gave a trichloride, and the holmium nitrate–hydroxide gave a nitrate–chloride. The cerium trichloride complex had the following IR absorptions (cm^{-1}), which are characteristic of the L^3 macrocycle free of anion absorptions: 3049 w, 3013 w, 2919 vvw, 1655 vvw, 1619 m, 1584 vs, 1490 s, 1455 m, 1378 m, 1273 s, 1237 m, 1214 w, 1167 s, 1120 vw, 1049 m, 1002 m, 879 w, 808 s, 785 m only partly resolved from strong adjacent peak, 767 s, 748 m only partly resolved from strong adjacent peak, 738 s, 656 vw, 594 vw, 579 vw, 532 m, 468 w.

Attempted Metal Extraction with 18-Crown-6. The lanthanum trinitrate and barium perchlorate complexes were heated to reflux with an excess of 18-crown-6 in acetonitrile for 4 h. After cooling and dilution of the mixture with diethyl ether, the original complexes were recovered unchanged in ca. 90% yields. In each case the mother liquor showed a strong purple glow upon UV irradiation, indicative of traces of 2,6-bis(2-benzimidazolyl)pyridine.

Luminescence Titration Measurements. A set of ethanol solutions were prepared containing a constant concentration of Eu–L^3 tritriflate (4.0×10^{-4} M) and increasing concentrations of the sodium salt of 4,4,4-trifluoro-1-(2-thienyl)butane-1,3-dione (Eu:diketone mole ratios: 0.1, 0.2, 0.3, 0.5, 1.0, 2.0, 3.0, 4.0, 5.0). The $^5D_0 \rightarrow {}^7F_2$ Eu transition was monitored at 616 nm (excitation, 375 nm) for all solutions. Relative emission intensities for increasing diketonate-to-Eu mole ratios were 0 for ratios 0–0.5, 1 for ratio 1, 7 for ratio 2, 10 for ratio 3, and 15 for ratios 4 and 5.

X-ray Measurements and Structural Determination. The crystal and refinement data for $[Sr_2(C_{26}H_{18}N_6)_2(CF_3SO_3)_4\cdot(H_2O)]$ (pale yellow transparent prisms) are summarized in Table IV. A prismatic crystal of dimensions $0.18 \times 0.22 \times 0.16$ mm was lodged in a Lindemann glass capillary and centered on a four-circle Philips PW 1100 diffractometer with graphite-monochromated Mo Kα radiation. The orientation matrix and preliminary unit cell dimensions were determined from 25 reflections found by mounting the crystal at random and varying each of the orientation angles χ and ϕ over a range of 120°, with $5 \leq \theta \leq 7°$. For the determination of precise lattice parameters, 25 strong reflections with $10 \leq \theta \leq 13°$ were considered. Integrated intensities for hkl reflections with $h = \pm 20$, $k = \pm 18$, and $l = 12$ were measured; two standard reflections, $-4,1,2$ and $-2,-1,3$, were monitored every 180 min. There were no significant fluctuations of intensities other than those expected from Poisson statistics.

The intensity data were corrected for Lorenz–polarization effects and for absorption by following the method of North et al.;[36] no correction was made for extinction. The structure was solved by using three-dimensional Patterson and Fourier techniques and refined with a blocked matrix (two blocks) because of the large number of variables. Anisotropic thermal parameters were assigned to all non-hydrogen atoms except C(140), F(14), F(15), and F(16), which were refined isotropically. Due to the disordering in the triflate moiety, the S–C distance was constrained to 1.72 (2) Å and the best refinement was obtained by using isotropic thermal parameters. The hydrogens of water, introduced in the positions given in the final Fourier distance map, were refined individually with fixed isotropic $U = 0.07$ Å^2.

Carbon-attached hydrogen atoms were introduced at the calculated positions and allowed to ride on the respective carbon atoms during the least-squares refinement ($d_{C-H} = 0.98$ Å and $U = 0.07$ Å^2). The function minimized was $\sum w\Delta^2$, with $\Delta = (|F_o| - |F_c|)$. Anomalous dispersion terms for Sr[37] were taken into account in the refinement. Atomic scattering factors were taken from ref 37. Data processing and computation utilized the SHELX 76 program package;[38] PLUTO[39] and ORTEP[40] were used for drawing. The refinement of the $[Sr_2(C_{26}H_{18}N_6)_2(CF_3SO_3)_4\cdot(H_2O)]$ complex converged at $R = 0.055$ and $R_w = 0.057$. Atomic fractional coordinates are given in Table V, bond lengths and angles in Table VI, and torsion angles in Table VII.

Results and Discussion

Synthesis of the Complexes. The nitrates of all lanthanide(III) ions promoted the cyclic 2:2 Schiff-base condensation of 2,6-diformylpyridine and 1,2-diaminobenzene, with the formation of metal complexes of the macrocyclic ligand L^3. Yields were quite high for the larger lanthanides (80–60% for La–Nd) and then gradually decreased and became minimal for the last members of the series (less than 5% for Lu). The size of the metal ion also affected the stoichiometry of the complexes; the larger lanthanides (La–Gd) formed trinitrates, $ML^3(NO_3)_3\cdot nH_2O$, with $n = 0$–4.5, whereas the smaller ions (Tb–Lu) yielded nitrate–hydroxide complexes, $ML^3(NO_3)_{3-x}(OH)_x\cdot nH_2O$ ($n = 0.5$–1.5). This change in stoichiometry most likely results from the steric requirements of the nitrate ligands, which become increasingly forbidding upon traversing the series, and also from the increased tendency of the smaller metal ions to hydrolyze. The triflates and acetates of the larger lanthanides also acted as templates for the synthesis of L^3 macrocycles, but yields were lower than for the corresponding nitrates. In general, the synthesis was favored by coordinating anions that formed sparingly soluble final products. This behavior contrasts with that of the corresponding L^1 systems, which were best synthesized as the extremely soluble diacetate–chlorides.[10]

A different approach to the synthesis of lanthanide–L^3 complexes has been described by Gray and Hart,[24] who obtained the trinitrates of La to Nd by metal exchange between the bimacrocyclic $Ba(L^3)_2(ClO_4)_2$ complex[33] and an excess of lanthanide nitrate in aqueous methanol. By carrying out the transmetalation reaction in anhydrous methanol and adding an excess of $LiNO_3$ or NaSCN, we extended Hart's method to Eu and the smaller lanthanides. The complexes thus formed were identical with those from the template synthesis, except that for the smaller lanthanides (Dy–Yb) nitrate–perchlorates or thiocyanate–perchlorates were

---

(36) North, A. C. T.; Philips, D. C.; Mathews, F. S. *Acta Crystallogr., Sect. A* **1968**, *24*, 351.

(37) *International Tables for X-Ray Crystallography*, 2nd ed.; Kynoch Press: Birmingham, England, 1974; Vol. 4, p 101.

(38) Sheldrick, G. M. *SHELX 76*; University of Cambridge: Cambridge, England, 1976.

(39) Motherwell, W. D. S.; Clegg, W. *PLUTO*; University of Cambridge: Cambridge, England, 1978.

(40) Johnson, C. K. *ORTEP II*; Oak Ridge National Laboratory Report ORNL-5138; Oak Ridge, TN, 1976.

Table V. Atomic Fractional Coordinates ($\times 10^4$) and U_{eq} ($\times 10^3$) with Esd's in Parentheses

atom	*x/a*	*y/b*	*z/c*	$U_{is/eq}$,[a] Å^2
Sr(1)	2771.8 (5)	2600.4 (5)	1394.8 (9)	41.6 (4)
O(1)	3233 (4)	1624 (5)	−520 (7)	81 (4)
S(1)	3948 (2)	2227 (2)	−678 (3)	60 (1)
O(2)	3992 (5)	3121 (4)	−143 (7)	91 (4)
O(3)	4597 (4)	2048 (5)	−375 (8)	90 (4)
C(30)	388 (1)	1992 (8)	−234 (1)	108 (9)
F(1)	3851 (5)	1178 (5)	−2938 (7)	123 (5)
F(2)	3310 (7)	2105 (7)	−2816 (8)	166 (8)
F(3)	4521 (6)	2529 (6)	−2632 (8)	162 (6)
O(4)	2386 (4)	3061 (5)	3599 (7)	78 (4)
S(2)	1776 (1)	3161 (2)	4250 (2)	51 (1)
O(5)	1932 (5)	4016 (4)	5144 (7)	88 (4)
O(6)	1072 (4)	2795 (5)	3426 (8)	101 (5)
C(40)	1669 (7)	2459 (8)	519 (1)	69 (6)
F(4)	1483 (5)	1628 (4)	4508 (7)	114 (4)
F(5)	2294 (5)	2686 (5)	5956 (7)	113 (4)
F(6)	1143 (4)	2527 (6)	5974 (8)	130 (5)
N(1)	2984 (4)	1515 (5)	2517 (7)	47 (4)
C(1)	3579 (5)	1807 (6)	3404 (9)	46 (5)
C(2)	3667 (6)	1314 (6)	412 (1)	58 (6)
C(3)	3097 (7)	498 (7)	393 (1)	73 (7)
C(4)	2482 (6)	208 (6)	306 (1)	63 (6)
C(5)	2429 (6)	716 (6)	233 (1)	56 (6)
C(6)	1810 (5)	422 (6)	138 (1)	56 (5)
N(2)	1741 (4)	878 (5)	711 (8)	49 (4)
C(7)	1141 (5)	539 (6)	−295 (9)	47 (5)
C(8)	727 (6)	−369 (6)	−92 (1)	69 (5)
C(9)	181 (6)	−629 (7)	−192 (1)	72 (6)
C(10)	6 (6)	−38 (9)	−233 (1)	84 (7)
C(11)	402 (5)	860 (7)	−173 (1)	68 (5)
C(12)	956 (5)	1139 (6)	−702 (9)	51 (5)
N(3)	1391 (4)	2050 (5)	−51 (7)	50 (4)
C(13)	1082 (5)	2602 (6)	90 (9)	52 (5)
C(14)	1507 (5)	3561 (6)	709 (8)	44 (4)
C(15)	1171 (5)	4164 (6)	649 (9)	53 (5)
C(16)	1600 (6)	5034 (6)	1206 (9)	55 (5)
C(17)	2312 (5)	5293 (6)	1803 (9)	51 (5)
C(18)	2608 (5)	4668 (6)	1816 (8)	42 (5)
N(4)	2206 (4)	3796 (4)	1259 (7)	43 (3)
C(19)	3377 (5)	4920 (6)	2421 (8)	47 (4)
N(5)	3668 (4)	4352 (4)	2344 (7)	43 (4)
C(20)	4428 (5)	4606 (6)	2847 (8)	43 (4)
C(21)	4986 (5)	5452 (6)	3060 (9)	52 (5)
C(22)	5715 (5)	5656 (6)	3523 (9)	53 (5)
C(23)	5933 (5)	5054 (7)	3812 (9)	58 (5)
C(24)	5408 (5)	4214 (7)	3601 (9)	57 (5)
C(25)	4668 (5)	3991 (6)	3140 (8)	42 (4)
N(6)	4092 (4)	3146 (4)	2925 (6)	40 (3)
C(26)	4155 (5)	2688 (6)	3593 (9)	46 (5)
Sr(2)	2289.0 (5)	7092.8 (5)	−2317.9 (8)	41.4 (3)
O(11)	1578 (4)	7471 (5)	−420 (7)	83 (4)
S(10)	1170 (1)	7404 (2)	629 (3)	62 (1)
O(12)	657 (4)	6536 (6)	489 (9)	114 (5)
O(13)	903 (5)	8112 (6)	1149 (8)	109 (6)
C(130)	1883 (7)	7586 (8)	187 (1)	75 (7)
F(11)	2439 (4)	8368 (4)	2148 (7)	109 (4)
F(12)	2236 (4)	7025 (4)	1494 (8)	110 (5)
F(13)	1616 (5)	7497 (8)	2875 (8)	164 (7)
O(14)	3363 (5)	7727 (5)	−3512 (8)	106 (5)
S(11)	3822 (2)	7682 (2)	−4462 (3)	66 (2)
O(15)	3582 (8)	6911 (6)	−5458 (9)	187 (8)
O(16)	4610 (5)	8002 (8)	−394 (1)	184 (9)
C(140)	3909	8560	−4964	214 (2)*
F(14)	4098 (7)	9279 (9)	−421 (1)	225 (5)*
F(15)	4125 (8)	8510 (9)	−601 (1)	253 (6)*
F(16)	3255 (9)	853 (1)	−533 (1)	262 (6)*
O(w)	2294 (5)	5862 (5)	−4438 (8)	76 (4)
N(11)	871 (4)	5828 (5)	−2910 (7)	45 (4)
C(101)	279 (5)	5960 (6)	−3392 (8)	49 (5)
C(102)	−446 (5)	5340 (7)	−3689 (9)	57 (5)
C(103)	−590 (5)	4545 (7)	−3478 (9)	55 (5)
C(104)	−7 (5)	4424 (6)	−2941 (9)	56 (5)
C(105)	715 (5)	5073 (6)	−2664 (8)	47 (5)
C(106)	1343 (5)	4941 (6)	−2096 (8)	48 (5)
N(12)	2012 (4)	5508 (5)	−1873 (7)	45 (4)
C(107)	2624 (5)	5341 (6)	−1387 (8)	45 (4)
C(108)	2599 (6)	4500 (6)	−1512 (8)	52 (5)
C(109)	3209 (6)	4374 (7)	−106 (1)	59 (6)
C(110)	3855 (6)	5087 (7)	−47 (1)	61 (6)
C(111)	3903 (5)	5927 (6)	−373 (9)	56 (5)
C(112)	3291 (5)	6071 (6)	−809 (8)	44 (4)
N(13)	3303 (4)	6910 (5)	−741 (7)	46 (4)
C(113)	3729 (5)	7584 (6)	170 (9)	50 (4)
C(114)	3795 (4)	8474 (6)	276 (9)	41 (4)
C(115)	4320 (5)	9205 (7)	1206 (9)	58 (5)
C(116)	4356 (6)	10032 (7)	132 (1)	67 (5)
C(117)	3865 (6)	10113 (6)	47 (1)	63 (5)
C(118)	3343 (5)	9353 (6)	−415 (9)	51 (5)
N(14)	3317 (4)	8542 (5)	−515 (7)	46 (3)
C(119)	2813 (6)	9432 (6)	−129 (1)	59 (5)
N(15)	2351 (4)	8769 (5)	−2169 (8)	48 (4)
C(120)	1887 (5)	8865 (6)	−3064 (9)	49 (5)
C(121)	2022 (6)	9642 (7)	−329 (1)	68 (6)
C(122)	1556 (7)	9701 (8)	−417 (1)	76 (7)
C(123)	957 (7)	8966 (8)	−491 (1)	74 (7)
C(124)	807 (6)	8180 (7)	−4705 (9)	63 (6)
C(125)	1258 (5)	8122 (6)	−3787 (9)	47 (5)
N(16)	1133 (4)	7323 (5)	−3507 (7)	47 (3)
C(126)	456 (5)	6802 (6)	−3618 (9)	51 (5)

[a] Asterisk indicates U_{is} value.

isolated, instead of nitrate–hydroxides. Yields ranged from ca. 80% for the larger lanthanides to ca. 30% for ytterbium.

Organic Byproducts of the Metal-Template Synthesis and Transmetalation Reaction. As the yields of macrocyclic complexes from the template synthesis gradually decreased along the lanthanide Series, proportionally increasing amounts of nonmacrocyclic organic byproducts were formed. In every case the major byproduct was 2,6-bis(2-benzimidazolyl)pyridine (Figure 1c), both as the white free base and as protonated salts or nonstoichiometric metal adducts. The formation of N-protonated organic byproducts has been observed in other metal-templated reactions[26] and results from the tendency of the hydrated lanthanide salts to hydrolyze to give acidic solutions. Minor quantities of 2,6-bis(2-benzimidazolyl)pyridine were also identified among the products of the transmetalation reactions of $Ba(L^3)_2(ClO_4)_2$.

When the condensation of 2,6-diformylpyridine and 1,2-diaminobenzene was carried out in the presence of cerium acetate or europium nitrate by using a 4:4:1 precursors-to-metal ratio, minor quantities of a different organic byproduct were obtained. On the basis of its ^1H and ^{13}C NMR spectra, this compound (molecular formula $C_{26}H_{18}N_6$) was assigned the highly condensed structure shown in Figure 1d. This compound is clearly different from the isomeric "twisted macrocycle" described by Bell and Guzzo[35] and is to our knowledge a previously unreported species.

Properties of the Macrocyclic Complexes. Appearance and Thermal Stability. With the exception of the Ce(III) derivatives, which are orange-brown, the lanthanide–L^3 complexes are bright yellow microcrystalline solids with high thermal stability. Any solvent present in the crystal lattice is released between 80 and 150 °C, but the metal–macrocycle entities remain unchanged up to 250 °C.

Infrared Spectra. The organic portions of the IR spectra (absorptions listed in the Experimental Section) are nearly identical for all lanthanide–L^3 complexes. They also closely resemble the spectra of $PbL^3(ClO_4)_2{\cdot}2H_2O$ (synthesis and crystal structure by Drew et al.[33]) and of $SrL^3(CF_3SO_3)_2{\cdot}0.5H_2O$, the crystal structure of which is discussed in a later section. The spectra show two sharp absorptions at ca. 1630 cm^{-1} (m) and ca. 1590 cm^{-1} (s), arising from the C=N stretching modes of the coordinated aromatic imine and pyridine groups, respectively. These two absorptions, identical with those observed for the complexes of the L^4 ligand,[26] are diagnostic of this type of macrocycle with *o*-phenylene side chains and pyridine head units. It should be noted that the spectrum of the bimacrocyclic $Ba(L^3)_2(ClO_4)_2$ complex

Table VI. Bond Lengths (Å) and Angles (deg) with Esd's in Parentheses

for Sr(1)		for Sr(2)	
(a) Strontium Environments			
Sr(1)–O(1)	2.640 (8)	Sr(2)–O(11)	2.555 (8)
Sr(1)–O(2)	2.955 (8)	Sr(2)–O(14)	2.560 (9)
Sr(1)–O(4)	2.531 (7)	Sr(2)–O(w)	2.633 (8)
Sr(1)–N(1)	2.682 (9)	Sr(2)–N(11)	2.727 (6)
Sr(1)–N(2)	2.779 (7)	Sr(2)–N(12)	2.796 (9)
Sr(1)–N(3)	2.761 (8)	Sr(2)–N(13)	2.759 (9)
Sr(1)–N(4)	2.677 (9)	Sr(2)–N(14)	2.731 (6)
Sr(1)–N(5)	2.739 (6)	Sr(2)–N(15)	2.800 (9)
Sr(1)–N(6)	2.715 (7)	Sr(2)–N(16)	2.764 (9)
O(1)–Sr(1)–O(2)	49.8 (2)	O(w)–Sr(2)–O(11)	145.2 (3)
O(1)–Sr(1)–O(4)	155.8 (3)	O(w)–Sr(2)–O(14)	69.8 (3)
O(2)–Sr(1)–O(4)	142.6 (2)	Sr(2)–O(11)–S(10)	161.2 (6)
Sr(1)–O(1)–S(1)	104.2 (4)	Sr(2)–O(14)–S(11)	154.8 (6)
Sr(1)–O(2)–S(1)	90.9 (4)	O(11)–S(10)–C(130)	103.2 (6)
Sr(1)–O(4)–S(2)	143.2 (5)	O(14)–S(11)–C(140)	105.9 (4)
O(1)–S(1)–C(30)	103.0 (6)		
O(4)–S(2)–C(40)	102.3 (6)		
Sr(1)–N(py)–C_{av}	120.7 (6)	Sr(2)–N(py)–C_{av}	121.2 (6)
Sr(1)–N(aliph)–C_{av}	119.6 (7)	Sr(2)–N(aliph)–C_{av}	120.1 (7)
(b) Ligand ($C_{26}H_{18}N_6$)			
N=C_{av}	1.27 (1)	N=C_{av}	1.27 (1)
N–C$(py)_{av}$	1.34 (1)	N–C$(py)_{av}$	1.34 (1)
C–C$(py)_{av}$	1.38 (2)	C–C$(py)_{av}$	1.38 (2)
C–C$(ph)_{av}$	1.39 (2)	C–C$(ph)_{av}$	1.38 (2)
C–C–C$(py)_{av}$	120 (1)	C–C–C$(py)_{av}$	120 (1)
C–C–C$(ph)_{av}$	120 (1)	C–C–C$(ph)_{av}$	120 (1)
(c) Ligands (CF_3SO_3)			
S(1)–O(1)	1.447 (7)	S(10)–O(11)	1.421 (8)
S(1)–O(2)	1.438 (8)	S(10)–O(12)	1.431 (9)
S(1)–O(3)	1.436 (9)	S(10)–O(13)	1.440 (9)
S(1)–C(30)	1.76 (2)	S(10)–C(130)	1.80 (1)
C(30)–F(1)	1.33 (2)	C(130)–F(11)	1.33 (1)
C(30)–F(2)	1.30 (2)	C(130)–F(12)	1.33 (2)
C(30)–F(3)	1.37 (2)	C(130)–F(13)	1.27 (2)
S(2)–O(4)	1.408 (8)	S(11)–O(14)	1.380 (9)
S(2)–O(5)	1.421 (7)	S(11)–O(15)	1.357 (9)
S(2)–O(6)	1.436 (8)	S(11)–O(16)	1.449 (9)
S(2)–C(40)	1.79 (2)	S(11)–C(140)	1.726 (4)
C(40)–F(4)	1.31 (1)	C(140)–F(14)	1.18 (1)
C(40)–F(5)	1.32 (2)	C(140)–F(15)	1.22 (2)
C(40)–F(6)	1.35 (2)	C(140)–F(16)	1.29 (2)
O–S–O_{av}	114.2 (5)	O–S–O_{av}	114.6 (7)
O–S–C_{av}	104.2 (6)	O–S–C_{av}	103.6 (6)
S–C–F_{av}	112 (1)	S–C–F_{av}	114 (1)
F–C–F_{av}	107 (1)	F–C–F_{av}	104 (1)

Table VII. Torsion Angles

atoms 1–2–3–4	2–3, Å	1–2–3, deg	1–2–3–4, deg
C(1)–N(1)–C(5)–C(6)	1.36 (1)	119.3 (9)	−179 (1)
N(1)–C(5)–C(6)–N(2)	1.41 (1)	118.0 (9)	−2 (2)
C(5)–C(6)–N(2)–C(7)	1.27 (2)	123 (1)	176 (1)
C(6)–N(2)–C(7)–C(12)	1.41 (1)	121.4 (9)	160 (1)
N(2)–C(7)–C(12)–N(3)	1.39 (2)	117.7 (9)	−1 (1)
C(7)–C(12)–N(3)–C(13)	1.43 (1)	116.5 (9)	−147 (1)
C(12)–N(3)–C(13)–C(14)	1.26 (2)	119.2 (9)	−177.4 (9)
N(3)–C(13)–C(14)–N(4)	1.48 (1)	122 (1)	−9 (2)
C(13)–C(14)–N(4)–C(18)	1.33 (1)	116.1 (9)	179.2 (9)
C(14)–N(4)–C(18)–C(19)	1.35 (1)	117.1 (9)	−179.9 (9)
N(4)–C(18)–C(19)–N(5)	1.46 (1)	116.8 (9)	5 (1)
C(18)–C(19)–N(5)–C(20)	1.27 (2)	121.4 (9)	175.2 (8)
C(19)–N(5)–C(20)–C(25)	1.41 (1)	121.0 (8)	158.9 (9)
N(5)–C(20)–C(25)–N(6)	1.41 (2)	119.5 (8)	−2 (1)
C(20)–C(25)–N(6)–C(26)	1.43 (1)	115.3 (8)	−152.1 (9)
C(25)–N(6)–C(26)–C(1)	1.27 (1)	119.2 (8)	−179.5 (9)
N(6)–C(26)–C(1)–N(1)	1.48 (1)	121.4 (9)	1 (1)
C(26)–C(1)–N(1)–C(5)	1.33 (1)	117.3 (9)	178.2 (9)
Sr(1)–O(1)–S(1)–C(30)	1.447 (7)	104.2 (4)	−134.4 (6)
Sr(1)–O(4)–S(2)–C(40)	1.408 (8)	143.2 (5)	121.8 (8)
C(101)–N(11)–C(105)–C(106)	1.34 (1)	116.9 (9)	−177.6 (9)
N(11)–C(105)–C(106)–N(12)	1.47 (2)	117.4 (9)	−2 (1)
C(105)–C(106)–N(12)–C(107)	1.27 (1)	121.3 (9)	−176.4 (9)
C(106)–N(12)–C(107)–C(112)	1.43 (1)	120.2 (9)	−161.5 (9)
N(12)–C(107)–C(112)–N(13)	1.40 (1)	117.0 (9)	1 (1)
C(107)–C(112)–N(13)–C(113)	1.42 (1)	117.7 (9)	152 (1)
C(112)–N(13)–C(113)–C(114)	1.27 (1)	118.7 (8)	117.5 (9)
C(113)–C(114)–N(14)–C(118)	1.32 (1)	116.7 (9)	117.6 (9)
C(114)–N(14)–C(118)–C(119)	1.35 (1)	118.4 (8)	179.8 (9)
N(14)–C(118)–C(119)–N(15)	1.46 (2)	118.6 (9)	−3 (2)
C(118)–C(119)–N(15)–C(120)	1.27 (1)	123 (1)	−175 (1)
C(119)–N(15)–C(120)–C(125)	1.41 (2)	121.6 (9)	−163 (1)
N(15)–C(120)–C(125)–N(16)	1.41 (1)	118.4 (9)	2 (1)
C(120)–C(125)–N(16)–C(126)	1.45 (1)	116.0 (9)	147 (1)
C(125)–N(16)–C(126)–C(101)	1.27 (1)	117.5 (9)	178 (1)
N(16)–C(126)–C(101)–N(11)	1.47 (2)	121 (1)	−8 (1)
C(126)–C(101)–N(11)–C(105)	1.36 (1)	116.3 (9)	−178.1 (9)
Sr(2)–O(11)–S(10)–C(130)	1.421 (8)	161.2 (6)	75 (2)
Sr(2)–O(14)–S(11)–C(140)	1.380 (9)	154.8 (6)	137 (1)

is virtually identical with that of the monomacrocyclic lead perchlorate complex. Apparently, the vibrational spectra of these species are not sensitive to the position of the metal ion relative to the macrocycle or to the details of the macrocycle configuration.

The absorptions of the counterions, listed in Table I, provide some useful structural information. In the trinitrate complexes, the two most intense nitrate absorptions—a strong, broad band at ca. 1440 cm^{-1} (ν_5) and a very strong, broad band with peaks at ca. 1340 and 1300 cm^{-1} (ν_1)—clearly identify these species as containing only coordinated nitrate groups. IR spectra do not generally allow a clear-cut distinction between monodentate and bidentate chelating nitrates, but the marked splitting of the ν_1 band suggests that both may be present. Species containing both types of NO_3^- groups have been reported for complexes of the L^2 macrocycle.[12] In the nitrate–hydroxide species, the spectra show both coordinated nitrate (ν_5 at ca. 1470 cm^{-1}, ν_1 at ca. 1345 cm^{-1}, and ca. 1280 cm^{-1}) and ionic nitrate (ν_3 at ca. 1380 cm^{-1}); the ν(OH) absorption appears as a broad band near 3250 cm^{-1}. In the nitrate–chloride of Ho, only two major nitrate absorptions remain, ν_5 at 1514 cm^{-1} and ν_1 at ca. 1280 cm^{-1}; their large separation suggests bidentate chelating coordination.

The triacetate complexes of La and Ce show the carboxylate absorptions as two rather symmetric and narrow bands, ν_a(COO) at ca. 1580 cm^{-1} and ν_s(COO) at ca. 1420 cm^{-1}, with the separation Δ = 160 cm^{-1}. This value of Δ is considered to be diagnostic[41] of ionic acetate (Δ = 164 cm^{-1} for $NaCH_3COO$) and contrasts with the much lower values observed in the L^2 complexes of Lu(III)[11] and Y(III),[14] known from X-ray analysis to contain bidentate chelating acetates. Larger values of Δ are instead observed for monodentate acetates.[41] The logical if unexpected inference is that in these complexes the acetates are ionic and the metal coordination sphere is completed by solvent molecules. The cerium diacetate–perchlorate complex, in which Δ = 113 cm^{-1}, most likely contains bidentate chelating acetates. In the tritriflate complexes of La and Eu, the higher frequency $\nu(SO_3)$ and $\nu(CF_3)$ absorptions overlap to give an extremely broad, structured band, which contrasts with the clearly separated absorptions of the strontium triflate complex and suggests the presence of both coordinated and ionic $CF_3SO_3^-$ groups. In all perchlorate complexes the ClO_4^- ions are clearly ionic. In the thulium thiocyanate–perchlorate species, the value of the ν(C≡N) absorption (2050 cm^{-1}) is indicative of N-bonded NCS^- groups.[14] Finally, all hydrated species show a broad ν(OH) absorption at ca. 3400 cm^{-1}, arising from the lattice water.

Nuclear Magnetic Resonance Spectra. The proton NMR spectra of the La complexes are reported in Table II, together with those of the strontium triflate and barium perchlorate species. All spectra exhibit the expected splitting patterns and chemical shifts; these vary with the metal ion and, to a lesser extent, with the counterion. The greatest variations are observed for the methine protons; for example, these occur at 9.96 ppm for lanthanum triflate and at 9.21 ppm for strontium triflate. All resonances of the bimacrocyclic barium perchlorate complex occur upfield compared to those of monomacrocyclic La and Sr com-

---

(41) Nakamoto, K. *Infrared and Raman Spectra of Inorganic and Coordination Compounds*; John Wiley and Sons: New York, 1986; pp 231–233.

plexes. For the methine resonance, the variation is as much as 1.17 ppm upfield relative to the strontium perchlorate analogue.

The proton NMR spectra of the paramagnetic praseodymium and europium trinitrate complexes in DMSO-d_6 gave the following chemical shifts (ppm vs TMS). $PrL^3(NO_3)_3$: 10.67, 2 H; 9.31, 1 H; 8.51, 2 H; 4.09, 2 H; 0.45, 2 H. $EuL^3(NO_3)_3$: 11.22, 2 H; 8.99, 2 H; 5.82, 1 H; 4.25, 2 H; −9.34, 2 H. The Pr values are in close agreement with those reported by Gray and Hart.[24] However, our experiments (at 300 MHz) did not resolve the coupling among the pyridine or benzene hydrogens, and for both metals all resonances appeared as broadened singlets. The resonances at 9.31 ppm for Pr and 5.82 ppm for Eu, of relative area 1, could be definitively assigned to the pyridine γ-hydrogens. Other assignments were not attempted, owing to the lack of coupling information and the inversion of resonances that may occur in paramagnetic species.

Carbon-13 NMR spectra of representative diamagnetic complexes are reported in Table III. In each case the expected resonances were observed; assignments were confirmed by heteronuclear correlation spectroscopy.

Solubility and Behavior in Solution. The solubility of the complexes in organic solvents was found to depend on the metal–counterion combination and was generally lower for the derivatives of the larger lanthanides. The "insoluble" complexes could be dissolved in warm methanol or ethanol containing a strong inorganic base, such as NaOH, but the resulting solutions were stable only for a limited time. In contrast, the lanthanide–L^3 moieties were extremely stable to acids and were recovered unchanged after prolonged contact with an excess of HCl in either water or methanol. In this respect, the L^3 complexes differed considerably from those of the similar 18-member macrocycle containing furan head units. The latter immediately decomposed in the presence of strong acids, forming the crystalline purple salts of the diprotonated metal-free ligand.[42]

All lanthanide–L^3 complexes underwent partial or complete anion metathesis when placed in contact with appropriate competing counterions. Reactions were practically instantaneous for the soluble complexes, showing the metal–anion association to be very labile. A similar behavior was reported for the lanthanide complexes of the L^2 and L^4 ligands.[10,11,26]

No metal release was observed when $LaL^3(NO_3)_3$ was refluxed for several hours with an excess of 18-crown-6 in methanol or acetonitrile. This behavior contrasts with that reported for the potassium triflate analogue, which was decomposed by 18-crown-6 with formation of the metal-free $C_{26}H_{18}N_6$ macrocycle, isolated in a "twisted" form.[35] We also found that the $Ba(L^3)_2(ClO_4)_2$ complex did not release the metal upon prolonged refluxing with 18-crown-6, even though it readily underwent transmetalation when gently heated in the presence of lanthanide(III) or potassium ions. This observation suggests that the transmetalation occurs via an initial coordination of the incoming metal ions to the available outer faces of the $[Ba(L^3)_2]$ sandwich. In contrast, no interaction can take place between 18-crown-6 and Ba(II), which is sheltered by the two parallel macrocycles.

Luminescence. None of the paramagnetic lanthanide–L^3 complexes exhibited visible luminescence upon UV irradiation. (Analytically pure samples occasionally showed a faint purple or bluish glow, due to traces of the highly luminescent ubiquitous byproducts, 2,6-bis(2-benzimidazolyl)pyridine and its protonated form.) In contrast, a few of the diamagnetic species exhibited a faint-to-moderate solid-state luminescence—orange-red for the strontium triflate and barium perchlorate complexes, yellow for the lanthanum nitrate, and yellow-green for the lanthanum triflate. The fact that the luminescence intensity of each sample does not decrease upon careful purification suggests that the phenomenon originates from the metal complex rather than from the presence of an impurity.

The Eu–L^3 triflate complex, which was not itself luminescent, immediately developed the typical red luminescence of Eu upon addition of the sodium salt of 4,4,4-trifluoro-1-(2-thienyl)butane-1,3-dione in methanol. Rapid, complete abstraction of the Eu from the macrocycle by the added diketonate ligand may be ruled out in view of the inertness of the metal–L^3 species. Partial abstraction also appears unlikely on the basis of luminescence titration experiments. This luminescence enhancement therefore must result from a partial or complete replacement of triflate ligands and/or coordinated solvent molecules by the luminescence-inducing β-diketonate, without disruption of the Eu–macrocycle moiety. A similar effect was observed for the Eu(III)–L^2 diacetate–chloride complex with a variety of chelating carboxylates.[43]

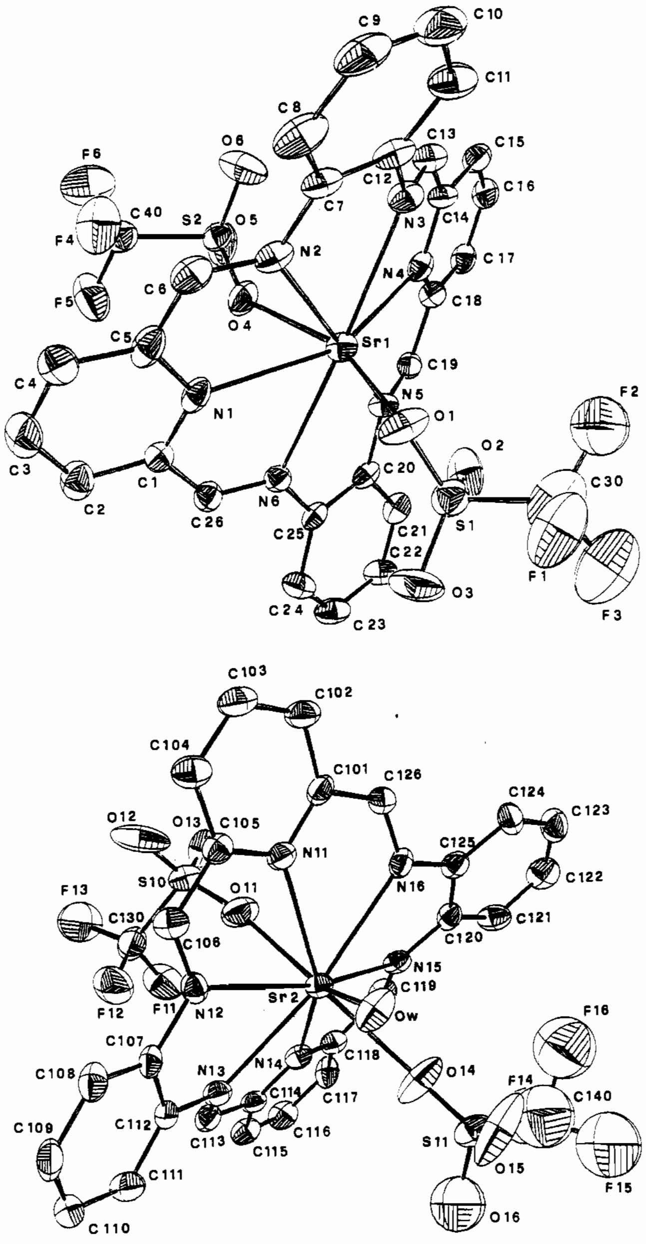

Figure 2. Structures of $SrL^3(CF_3SO_3)_2$ (**1**) (top) and $SrL^3(CF_3SO_3)_2(H_2O)$ (**2**) (bottom).

X-ray Crystal Structure of the Strontium(II) Triflate Complex. The structure contains two distinct molecules, **1** and **2** (Figures 2 and 3), present in a 1:1 ratio. A view of the unit cell is shown in Figure 4. Each molecule contains a Sr(II) ion linked to the

---

(42) Nelson, S. M.; Esho, F. S.; Drew, M. G. B. *J. Chem. Soc., Dalton Trans.* **1983**, 1857.

(43) De Cola, L.; Smailes, D. L.; Vallarino, L. M. *Abstracts of Papers*, 189th National Meeting of the American Chemical Society, Miami Beach, FL, April 1985; American Chemical Society: Washington, DC, 1985; INOR 149.

(44) Batchelor, R. J.; Ruddick, J. N. R.; Sams, J. R.; Aubke, F. *Inorg. Chem.* **1977**, *16*, 1414.

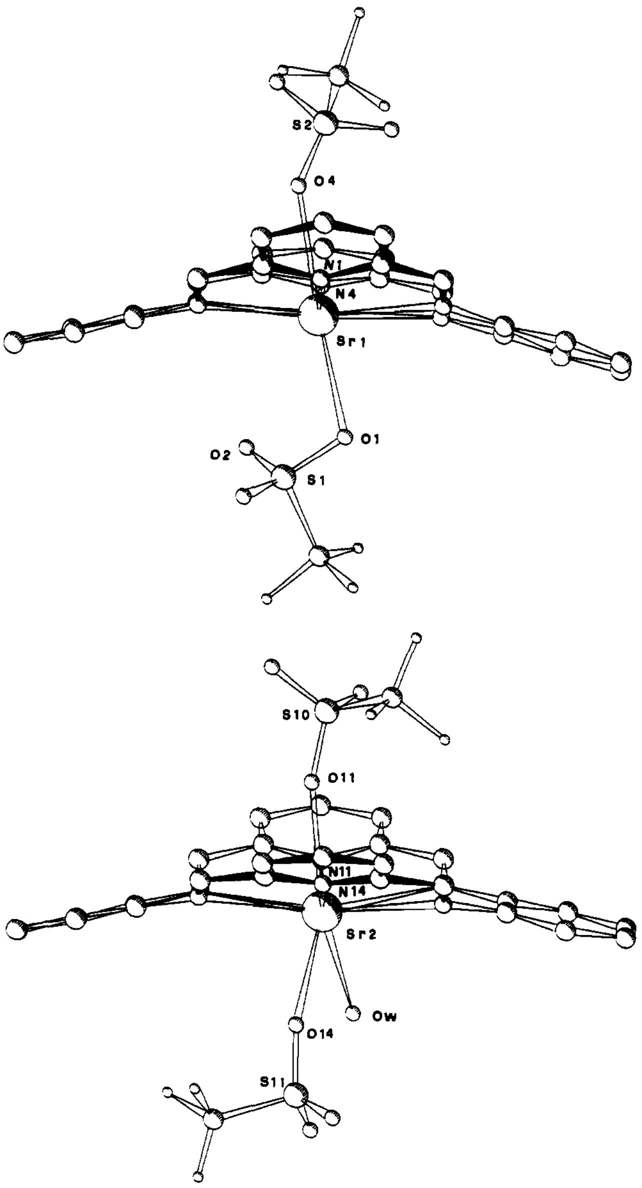

Figure 3. Views of **1** (top) and **2** (bottom) along the quasi-planar macrocyclic ligand.

six N-donor atoms of an equatorial $C_{26}H_{18}N_6$ macrocyclic ligand. In addition, **1** contains a monodentate triflate and an asymmetrically chelating bidentate triflate on opposite sides of the macrocycle; **2** has a monodentate triflate on one side and a second monodentate triflate and a coordinated water molecule on the other.

In both **1** and **2** the O atoms of the lone monodentate triflate occupy a pseudoaxial position with respect to the macrocycle, but the Sr–O distance is slightly shorter in **1** (Sr(1)–O(4) = 2.531 (7) Å) than in **2** (Sr(2)–O(11) = 2.555 (8) Å). Conversely, the Sr–O distances on the opposite side are shorter in **2** (Sr(2)–O(14) = 2.560 (9) Å, Sr(2)–O(w) = 2.633 (8) Å) than in **1** (Sr(1)–O(1) = 2.640 (8) Å, Sr(1)–O(2) = 2.955 (8) Å). Here the two values for the asymmetrically chelated triflate differ by more than 0.3 Å. The lengths of the Sr–O bonds on the two-oxygen side of the macrocycle apparently affect the corresponding Sr–N bond lengths. In **2**, where these Sr–O distances are shorter, the average Sr–N distances (Sr(2)–N(py) = 2.729 Å, Sr(2)–N(imine) = 2.780 Å) are longer than in **1** (Sr(1)–N(py) = 2.680 Å, Sr(1)–N(imine) = 2.749 Å).

The conformations of the macrocyclic ligands are illustrated in Figure 3, which shows views of **1** and **2** along the planes formed by the Sr ion and the two midpoints of the "basal" bonds (e.g. C(7)–C(12) and C(20)–C(25)) of the respective benzene rings. In each case the macrocycle is folded, with the two pyridine rings directed away from the hemisphere containing the pseudobidentate triflate (in **1**) or the monodentate triflate and the water molecule (in **2**). In molecule **1** the angle between the planes of the pyridine rings is 141.9 (3)°, and that between the planes of the two *o*-phenylene rings is 30.4 (3)°. The corresponding values for **2** are 146.1 (3)° and 154.6 (3)°, respectively. In each case the folding is rather asymmetric, but the greater distortions are found in **1**, where the triflate oxygen O(2), characterized by the long Sr–O distance, appears to exert greater steric hindrance than the coordinated water in **2**. The angle formed by the Sr(1)–O(1)–O(2) plane with the N(1) pyridine ring is 84.3 (2)°, while that with the N(4) pyridine ring is 112.4 (3)°. The corresponding angles in **2**, i.e. those formed by the Sr(2)–O(14)–O(w) plane with the N(14) and N(11) pyridine rings, are 85.6 (3) and 97.2 (2)°, respectively. In both **1** and **2** the six N-donor atoms of the macrocycle constitute a roughly planar hexagonal arrangement, with the Sr atom slightly displaced out of this plane toward the hemisphere containing the two O-donor atoms. The deviations of the N atoms from the calculated mean plane range from +0.264 (8) to −0.354 (8) Å for **1** and from +0.232 (8) to −0.293 (7) Å for **2**. The out-of-plane Sr displacement is 0.299 (2) Å for **1** and 0.480 (2) Å for **2**.

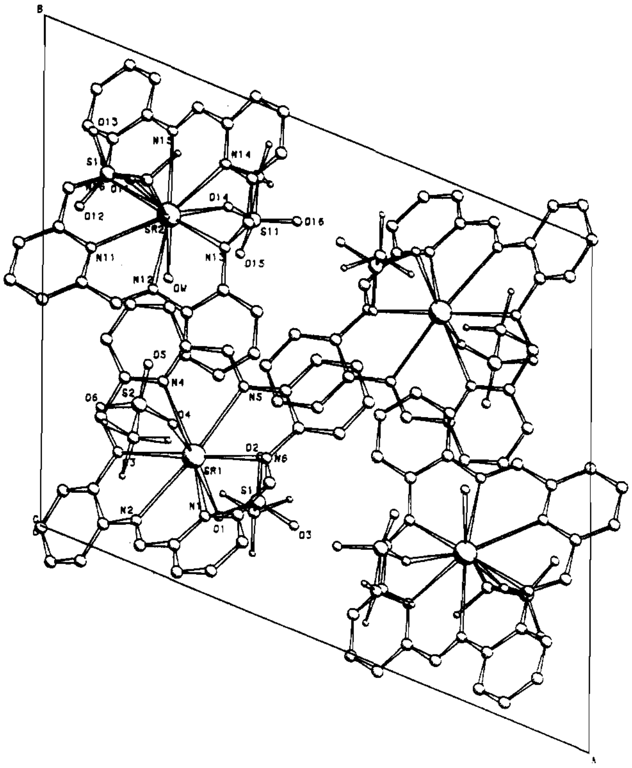

Figure 4. Unit cell of $[Sr_2(C_{26}H_{18}N_6)_2(CF_3SO_3)_4 \cdot H_2O]$.

The only interaction between molecule **1** and molecule **2** is the hydrogen bonding between one of the H atoms of the water molecule coordinated to Sr(2) and one of the (free) O atoms of the monodentate triflate coordinated to Sr(1). The relevant distances (Å) are O(w)–H(2w) = 0.90 (12), O(w)···O(5)′ = 2.89 (1), and H(2w)···O(5)′ = 2.11 (10); the O(w)–H(2w)···O(5)′ angle is 145 (9)° (the prime indicates symmetry coordinates *x*, *y*, *z* − 1). This interaction may be responsible for the fact that the bending of the strontium–triflate (monodentate) linkage at the O-donor atom is greater in molecule **1** (Sr(1)–O(4)–S(2) = 143.2 (5)°) than in molecule **2** (Sr(2)–O(11)–S(10) = 161.2 (6)° and Sr(2)–O(14)–S(11) = 154.8 (6)°).

The departure of the L^3 macrocycle from planarity in this Sr complex is sufficient to prevent extensive conjugation among the four aromatic sections. This situation is somewhat similar to that found in the Pr(III) complex of the tetramethyl analogue L^4, of formula $[PrL^4(NO_3)_2(CH_3OH)]ClO_4$, where, however, the folding is much more pronounced (py–py dihedral angle, 113.0°; bz–bz dihedral angle, 112.1°). In the L^4 complex Pr is 11-coordinate;

it is linked to a bidentate chelating nitrate on one side of the macrocycle and to a second bidentate chelating nitrate and a methanol molecule on the other side. Thus, it becomes difficult to determine whether the greater degree of planarity of the Sr–L^3 complex compared to the Pr–L^4 analogue results from the lower metal coordination number, from the absence of the four sterically hindering methyl groups, or from a combination of both factors. The structures of only two other complexes of L^3, those of the isomorphous pair $[CdL^3(H_2O)(ClO_4)](ClO_4)\cdot CH_3OH$ and $[PbL^3(H_2O)](ClO_4)_2\cdot H_2O$, have been reported.[33] In the Cd complex the metal ion is 8-coordinate and has an approximate hexagonal-bipyramidal geometry, being bonded to a water molecule and a perchlorate oxygen atom in the axial positions. In the Pb complex, the two perchlorates are ionic and the water molecule is axially coordinated to the metal on one side of the macrocycle, leaving the opposite side completely free or, rather, as the authors suggest, occupied by a stereochemically active Pb lone pair. The macrocycle is described as nearly planar, giving further support to the idea that the steric hindrance of the axially coordinated ligands has a determining influence on the macrocycle conformation.

Acknowledgment. We wish to thank Mr. James D. Spivey for the electron microscope examinations and Mr. Mark A. Benvenuto (Department of Chemistry, University of Virginia) for the measurement of mass spectra. We also acknowledge the financial support of a VCU Grant-In-Aid, of Coulter Electronics, Hialeah, FL, and of NATO Bilateral Project No. 184-85.

Supplementary Material Available: Tables IA, IIA, and IVA, listing crystal data, fractional hydrogen coordinates, and C, H, and N microanalyses (3 pages); Table IIIA, listing structure factors (18 pages). Ordering information is given on any current masthead page.

Contribution from the Department of Chemistry,
University of Hawaii, Honolulu, Hawaii 96822

Unusual Reversible Dimerization of a μ-Pyridine-2-thiolato (pyS) Complex: Crystal Structure of $Pd_2(\mu\text{-}N\text{–}S\text{-}\eta^2\text{-pyS})_2Cl_2(PMe_3)_2$

John H. Yamamoto, Wesley Yoshida, and Craig M. Jensen*

Received June 1, 1990

Reaction of $[PdCl(PMe_3)(\mu\text{-}Cl)]_2$ with sodium pyridine-2-thiolate in ethanol gives rise to $Pd_2(\mu\text{-}N\text{–}S\text{-}\eta^2\text{-pyS})_2Cl_2(PMe_3)_2$ (**1**). Variable-temperature ^1H and $^{31}P\{^1H\}$ NMR spectra of **1** indicate fluxional behavior associated with the bridging pyS ligands. The dramatic temperature-dependent shift in the equilibrium position of the interconverting species demonstrates that a large entropy change is associated with the dynamic process. From the ratios of the changing integrated intensities of the signals in the $^{31}P\{^1H\}$ NMR spectra over the −30 to +70 °C temperature range, values of $\Delta H = 26 \pm 1$ kJ mol^{-1}, $\Delta S = 75 \pm 3$ J K^{-1} mol^{-1} and $\Delta G_{293} = 4$ kJ mol^{-1}, for the fluxional process, can be calculated while similar analysis of the signals for the PMe_3 protons in ^1H NMR spectra over the 20–80 °C range are indicative of similar energetic values of $\Delta H = 29 \pm 1$ kJ mol^{-1}, $\Delta S = 87 \pm 4$ J K^{-1} mol^{-1} and $\Delta G_{293} = 4$ kJ mol^{-1}. The signals for the trimethylphosphine protons are observed to coalesce at 97 °C, and this thus allows calculation of a ΔG^* of 72 kJ mol^{-1} for the dynamic process. Variable-temperature $^{13}C\{^1H\}$ NMR spectroscopy indicates that the dynamic process involves interconverting η^2-pyS complexes. Molecular weight determinations by measurement of carbon tetrachloride boiling-point elevation demonstrate that a monopalladium complex is the predominant species present at elevated temperatures. The crystal and molecular structure of **1**·EtOH has been determined. Crystallographic data for **1**·EtOH: orthorhombic *Pbca*, $Z = 8$, $a = 12.588\ (4)$ Å, $b = 20.08\ (1)$ Å, $c = 20.45\ (1)$ Å, $V = 5170\ (5)$ Å^3, $\rho_{calcd} = 1.737$ g/cm^3.

Introduction

Complexes containing pyridine-2-thiolate, pyS, ligands in a variety of bridging coordination modes have recently been reported.[1-3] Fluxional behavior involving bridging pyS ligands has been noted[2,3a] for several of these complexes. Mechanisms involving eight-membered ring inversion as well as cleavage of a Pd–N bond followed by rotation about a Pd–S bond were considered by Deeming[2] for the exchange of diastereotopic methyl groups in $Pd_2[2\text{-(dimethylamino)phenyl}]_2(\mu\text{-}N\text{–}S\text{-}\eta^2\text{-pyS})_2$, with the latter mechanism considered to be more likely. Alternatively, Oro[3a] has proposed a mechanism involving intermediate μ-*S*-η^2-coordinated pyS ligands for intermolecular exchange of carbonyl groups in $Rh_2(pyS)_2(CO)_2$ and proton exchange processes in $Rh_2(pyS)_2(olefin)_2$ complexes.

We have isolated $Pd_2(\mu\text{-}N\text{–}S\text{-}\eta^2\text{-pyS})_2Cl_2(PMe_3)_2$ (**1**) and determined its molecular structure through a single-crystal X-ray diffraction study. In solution, **1** is seen by ^1H, ^{13}C, and ^{31}P NMR spectroscopy to establish a highly temperature-dependent equilibrium with a second species. Our variable-temperature NMR studies and molecular weight determinations indicate that a rapid equilibrium is established between the dimetallic complex, **1**, and a monometallic $Pd(pyS)Cl(PMe_3)$ complex. The (μ-halo)dipalladium complexes, $Pd_2(\mu\text{-}X)_2X_2(PR_3)_2$ (X = Cl, Br) have long been believed[4] to undergo rapid dimer–monomer interconversion in solution. However, monomeric intermediates have not been considered in the fluxional behavior of dimetallic μ-η^2-pyS complexes due to the high thermal stability that has generally been found[5] for monomeric pyS complexes. We herein report the synthesis and molecular structure of **1** along with the results of our studies of this complex by variable-temperature ^1H, ^{31}P, and ^{13}C NMR spectroscopy.

---

(1) (a) Kinoshita, I.; Yasuba, Y.; Matsumoto, K.; Ooi, S. *Inorg. Chim. Acta* **1983**, *80*, L13–L14. (b) Deeming, A. J.; Meah, M. N.; Dawes, H. M.; Hursthouse, M. B. *J. Organomet. Chem.* **1986**, *299*, C25–C28. (c) Umakoshi, K.; Kinoshita, I.; Ooi, S. *Inorg. Chim. Acta* **1987**, *80*, L41–L42. (d) Deeming, A. J.; Meah, M. N.; Bates, P. A.; Hursthouse, M. B. *J. Chem. Soc., Dalton Trans.* **1988**, 235–238. (e) Deeming, A. J.; Karim, M.; Bates, P. A.; Hursthouse, M. B. *Polyhedron* **1988**, *7*, 1401–1403. (f) Padilla, E. M.; Yamamoto, J. H.; Jensen, C. M. *Inorg. Chim. Acta* **1990**, *174*, 209–215.

(2) Deeming, A. J.; Meah, M. N.; Bates, P. A.; Hursthouse, M. B. *J. Chem. Soc., Dalton Trans.* **1988**, 2193–2199.

(3) (a) Ciriano, M. A.; Viguri, F.; Torrente-Perez, J. J.; Lahoz, F. J.; Oro, L. A.; Tiripicchio, A.; Tiripicchio-Camellini, M. *J. Chem. Soc., Dalton Trans.* **1990**, 25–32. (b) Ciriano, M. A.; Torrente-Perez, J. J.; Viguri, F.; Lahoz, F. J.; Oro, L. A.; Tiripicchio, A.; Tiripicchio-Camellini, M. *J. Chem. Soc., Dalton Trans.* **1990**, 1493–1502.

(4) (a) Chatt, J.; Venanzi, L. M. *J. Chem. Soc.* **1957**, 2445. (b) Cotton, F. A.; Wilkinson, G. *Advanced Inorganic Chemistry*, 4th ed.; John Wiley: New York, 1980; p 952.

(5) Deeming, A. J.; Meah, M. N.; Randle, N. P.; Hardcastle, K. I. *J. Chem. Soc., Dalton Trans.* **1989**, 2211–2216.

0020-1669/91/1330-1353$02.50/0 © 1991 American Chemical Society